Stacked Structures for Assembling Multiple Organic Photovoltaic Devices

2012 Appl. Phys. Express 5 072301

(http://iopscience.iop.org/1882-0786/5/7/072301)

Applied Physics Express **5** (2012) 072301
http://dx.doi.org/**10.1143/APEX.5.072301**

Stacked Structures for Assembling Multiple Organic Photovoltaic Devices

Wei-Chi Chen, Shang-Chieh Chien, Fang-Chung Chen*, and Chain-Shu Hsu[1]

Department of Photonics and Display Institute, National Chiao Tung University, Hsinchu 30010, Taiwan
[1]*Department of Applied Chemistry, National Chiao Tung University, Hsinchu 30010, Taiwan*

Received March 6, 2012; accepted June 3, 2012; published online June 25, 2012

We have prepared semitransparent organic photovoltaic devices for constructing stacked structures. Through the study of the thickness effect of the photoactive layer, we found that sophisticated optimization of device matching was not required for achieving high performance while the subcells were connected in parallel. The results suggest that the stacked structure might be able to provide the other approach for assembling multiple devices while current matching between the subcells cannot be easily obtained. © 2012 The Japan Society of Applied Physics

Organic photovoltaic devices (OPVs) are attracting increasing attention because they have many advantageous properties, including mechanical flexibility, light weight, and low-cost fabrication.[1–5] At present, OPVs based on the concept of bulk heterojunction (BHJ) show power conversion efficiencies (PCEs) up to ~7%, rendering OPVs as a promising next-generation solar energy conversion platform.[1,2] One of the key issues toward achieving high efficiencies is sufficient photon absorption.[3–5] Nevertheless, the low mobility of organic materials limits the thickness of the photoactive layer; the use of a thicker layer usually leads to increased device series resistances, thereby decreasing the PCEs. One method of solving this problem is to produce tandem cells.[4–6] The fabrication procedure for the multiple junctions, however, usually involves sophisticated processing, especially for the intermediate connecting layer(s). The yield of the tandem cells is also lower than that of single-junction cells.

An alternative method of realizing multijunction OPVs is the use of a multiple-device stacked structure.[7] Shrotriya *et al.* superimposed one semitransparent device onto another conventional cell, and connected them either in series or in parallel. As a resulting of stacking, the PCE can be doubled compared with that of a single cell. Nevertheless, relevant reports concerning such stacked structure of OPVs remain rare.[7,8] Herein, we analyzed stacked structures for OPVs incorporating a blend of poly(3-hexylthiophene) (P3HT) and [6,6]-phenyl-C_{61}-butyric acid methyl ester (PCBM) and found that the possibility of parallel connections could provide the other way for improving the efficiency if the current matching cannot be easily achieved.

The device structure of the semitransparent devices is shown in Fig. 1(a). The devices were fabricated on indium–tin-oxide (ITO)-coated glass substrates. Prior to the deposition of the organic layers, the substrate surface was treated with UV ozone. Then, the anodic buffer layer, poly(3,4-ethylenedioxythiophene):poly(styrene sulfonate) (PEDOT:PSS), was spin-coated on the ITO substrates. After annealing of the PEDOT:PSS film at 120 °C for 1 h, the photoactive layer, consisting of P3HT and PCBM (1 : 1, w/w) dissolved in 1,2-dichlorobenzene, was spin-coated on top of the PEDOT:PSS layer. The prepared polymer thin film underwent "solvent annealing" for more than 2 h.[9,10] Before the metal deposition, the substrate was further thermally annealed at 110 °C for 15 min. For conventional devices, the metals, Ca (30 nm) and Al (100 nm) were deposited to form the bilayer cathode. For semitransparent devices, the transparent cathode structure was deposited through sequential thermal evaporation of layers of lithium fluoride (LiF), aluminum (Al), and silver (Ag). The current density–voltage (J–V) curves were measured using a Keithley 2400 source-measure unit. The absorption/transmission spectra were obtained using a Perkin-Elmer Lambda 650 spectrometer. The photocurrent was obtained while the OPV was illuminated with a Thermal Oriel 150W solar simulator (AM1.5G).

The multilayer structure LiF (0.5 nm)/Al (1.5 nm)/Ag (10–20 nm) was chosen as the semitransparent cathode. The LiF/Al structure has been reported as an effective contact at the cathodes.[7,11] The Ag layer was used due to its high electrical conductivity and long skin depth.[8] Figure 1(b) displays the transmission spectra for the semi-

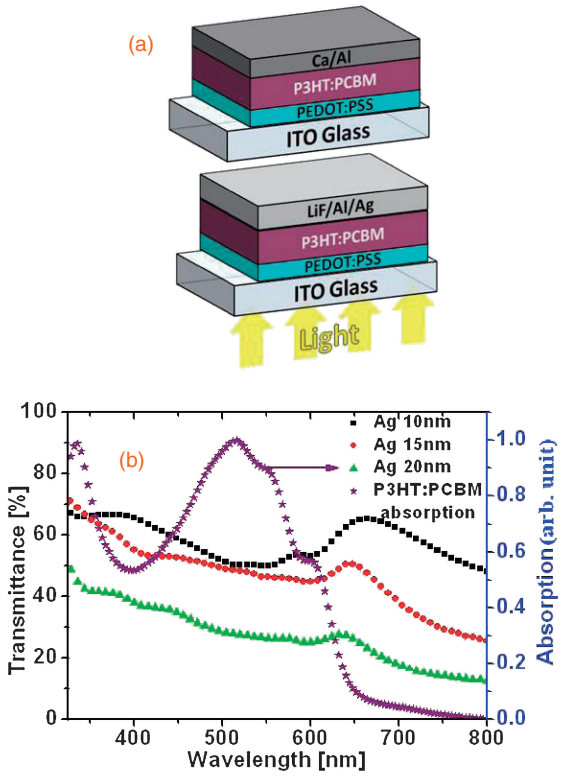

Fig. 1. (a) Architectures of the semitransparent organic photovoltaic devices and the stacked structure. (b) Transmittance spectra of the semitransparent cathodes of various Ag thicknesses. The absorption spectrum of the P3HT:PCBM thin film is also displayed for comparison. Note that the structure glass/ITO/PEDOT:PSS/P3HT:PCBM was used as the 100% transmission baseline during the transmittance measurements.

*E-mail address: fcchen@mail.nctu.edu.tw

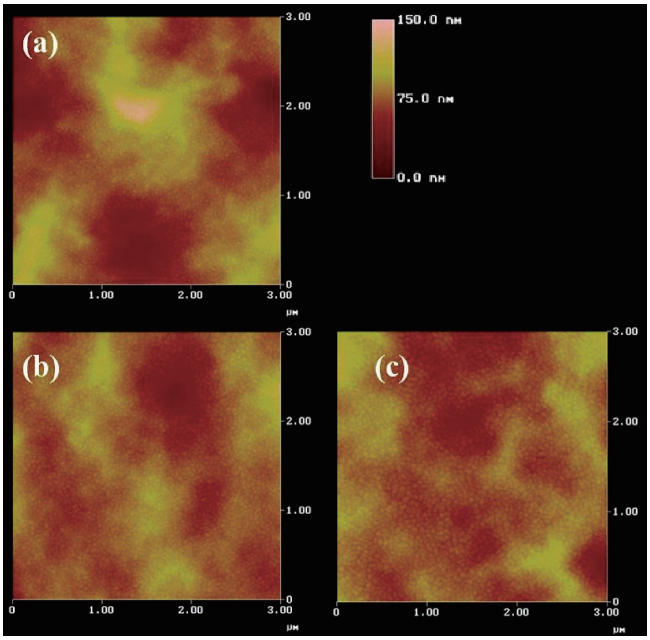

Fig. 2. Tapping mode AFM images ($3 \times 3\,\mu m^2$) of the Ag layers with various thicknesses. The Ag layers were deposited on the substrates with the structure ITO/PEDOT:PSS/P3HT:PCBM/LiF (0.5 nm)/Al (1.5 nm). The thickness of the Ag layer was (a) 10; (b) 15; (c) 20 nm.

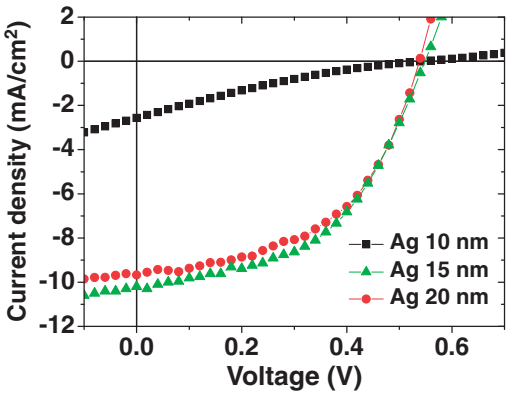

Fig. 3. *J–V* characteristics of the semitransparent OPVs prepared with different thicknesses of Ag layer.

transparent cathodes of various Ag thicknesses. From the figure, we can clearly see that the main absorption peak of the P3HT:PCBM film was located between 400 and 600 nm. Meanwhile the semitransparent structures exhibited high transmittances in the same spectral range. When the thickness of the Ag layer was 15 nm, the average transmittance values in the visible range was *ca.* 50%, suggesting that this multilayer structure was one promising candidate for the electrodes of semitransparent OPVs.

The surface morphologies of the Ag layers were further examed by using atomic force microscopy (AFM); the results are shown in Fig. 2. From the figures, we can clearly see some individual Ag nanoparticles (NPs) while the experimental "thickness", obtained from the thickness monitor of the thermal evaporator, was 10 nm [Fig. 2(a)]. The diameter of the Ag NPs was increased with the film thickness and the NPs and gradually coalesced to form a thin film [Figs. 2(b) and 2(c)]. Because of the apparent appearance of the Ag NPs for the 10 nm thick Ag layer, the transmittance spectrum was different. We can see that it contained an additional absorption peak at around 500 nm, which we attributed to the surface plasmon absorption of the Ag NPs.

Figure 3 reveals the *J–V* characteristics of the semitransparent devices obtained under illumination with simulated solar light. Although the device employing the 10-nm-thick Ag layer had the highest transmittance values, it exhibited poor device performance, with an open-circuit voltage (V_{oc}) of 0.55 V, a short-circuit current (J_{sc}) of 2.56 mA cm^{-2}, and a fill factor (FF) of 19%, resulting in a PCE of 0.27%. The lower FF and PCE were due to the low conductivity of the thin Ag layer. We also calculated the device series resistances (R_s) from the device *J–V* curves measured in the dark. The R_s was decreased significantly from 36.6 to 5.3 Ω cm^2 when the thickness of the Ag layer was increased from 10 to 15 nm, suggesting that the conductivity of the Ag layer affected the electrical properties dramatically. As a result, the J_{sc} and FF were improved to 10.1 mA cm^{-2} and 50%, respectively. The PCE was increased to 2.75%. For the device fabricated with a 20-nm-thick Ag, the device efficiency was somehow degraded to 2.60%, presumably due to the decreased shunt resistance (R_p); the shunt resistance was decreased from 2.2×10^4 to 2.0×10^3 Ω cm^2 while the thickness of the Ag layer was increased from 15 to 20 nm. We inferred that the diffusion of the Ag atoms to the organic photoactive layer might reduce the device R_p.

The stacked structure was implemented through stacking the transparent device onto a conventional device; the back cell could absorb the photons passing through the transparent device. The two subcells were connected either in series or in parallel. Figure 4(a) shows the *J–V* curves of the individual subcells and the stacked devices. Because most photons were absorbed by the transparent device, the back cell exhibited a smaller photocurrent (i.e., 1.43 mA cm^{-2}). The V_{oc} and FF were 0.49 V and 63%, respectively, resulting in a PCE of 0.43%. When the devices were connected in series, the V_{oc} was increased to 1.03 V, which was close to the sum of the voltages of the single cells. Furthermore, according to the well-known Kirchhoff's law, the current in the same loop should be identical. Hence, although the semitransparent device exhibited higher J_{sc}, the photocurrent of the two cells connected in series was limited by the back cell, thereby leading to a low PCE of 1.07%, which was lower than that of the semitransparent device. On the other hand, when the subcells were connected in parallel, the photocurrent was significantly improved to 11.5 mA cm^{-2}. The V_{oc} and FF were 0.53 V and 52%, respectively. Although the voltage was limited by the backcell, an improved PCE of 3.17% was still obtained.

The thickness of the photoactive layers significantly affected the device performance for both types of device. Therefore, we further reduced the thickness of the semitransparent devices to investigate the thickness effect on the performance of the stacked structures. Figure 4(b) shows the *J–V* curves of the individual subcells and the stacked devices. The thickness of the semitransparent device was reduced to 100 nm, thereby allowing more photons to pass through the semitransparent cell. Because the back cell

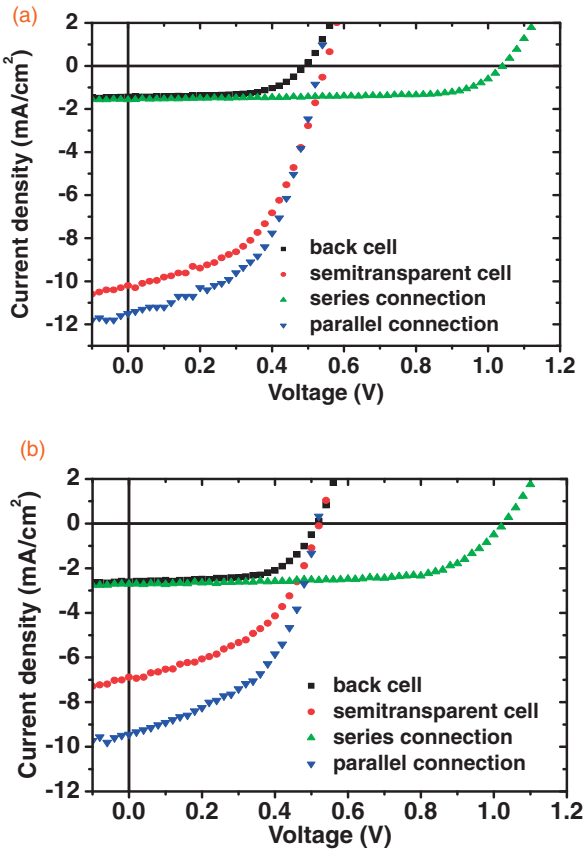

Fig. 4. *J*–*V* curves of the semitransparent device, the conventional device, and the stacked structures connected either in series or in parallel. The thicknesses of the photoactive layer of the semitransparent device were (a) 220 and (b) 100 nm.

could absorb more photons, the J_{sc} was increased to 2.61 mA cm^{-2}, resulting in an increased PCE of 0.83%. However, because the thinner photoactive layer harvested less numbers of photons, the semitransparent device exhibited a lower efficiency (1.70%). Therefore, although the PCEs of the stacked structure connected in series and in parallel were increased to 1.87 and 2.36%, respectively, the efficiency was still lower than that of the optimized single-junction semitransparent device (i.e., 2.75%).

From the above results, we can see that the principle behind the stacked structure might be different from that of the conventional tandem cells. In conventional tandem OPVs, because the subcells are naturally connected in series, the current matching phenomenon between the subcells plays an important role in determining the device efficiency.[6)] However, in stacked structures, as shown in Fig. 4(b), the better current matching obtained after the optimization of the photoactive layer still led to a lower PCE. Fortunately, the subcells for stacked structures can still be connected in parallel, which does not require photocurrent matching between the subcells. Further, considering the fact that the variation of photovoltages of OPVs is relatively smaller than that of the photocurrent to the intensity of the incident light,[6,12)] the possibility of parallel connections for the stacked structure could provide a better assembling method for multiple cells if current matching could not be easily achieved.

In conclusion, we have fabricated semitransparent OPVs based on P3HT and PCBM for constructing stacked structures. The thickness effect of the photoactive layer was studied, and we realized that the stacked structure might be able to provide the other approach for connecting two single-junction OPVs while the matching between the subcells could not be easily achieved. Finally, we foresee that this structure might be of further use for other materials, such as polymers containing different band gaps, to achieve higher efficiencies.

Acknowledgments We thank the National Science Council of Taiwan (NSC 101-3113-E-009-005 and NSC 100-2221-E-009-082) and the Ministry of Education of Taiwan (through the ATU program) for financial support.

1) S. H. Park, A. Roy, S. Beaupré, S. Cho, N. Coates, J. S. Moon, D. Moses, M. Leclerc, K. Lee, and A. J. Heeger: Nat. Photonics **3** (2009) 297.
2) H. Y. Chen, J. Hou, S. Zhang, Y. Liang, G. Yang, Y. Yang, L. Yu, Y. Wu, and G. Li: Nat. Photonics **3** (2009) 649.
3) J. L. Wu, F. C. Chen, Y. S. Hsiao, F. C. Chien, P. Chen, C. H. Kuo, M. H. Huang, and C. S. Hsu: ACS Nano **5** (2011) 959.
4) J. Y. Kim, K. Lee, N. E. Coates, D. Moses, T. Q. Nguyen, M. Dante, and A. J. Heeger: Science **317** (2007) 222.
5) S. Sista, Z. Hong, L. M. Chen, and Y. Yang: Energy Environ. Sci. **4** (2011) 1606.
6) F. C. Chen and C. H. Lin: J. Phys. D **43** (2010) 025104.
7) V. Shrotriya, E. H. E. Wu, G. Li, Y. Yao, and Y. Yang: Appl. Phys. Lett. **88** (2006) 064104.
8) R. F. Bailey-Salzman, B. P. Rand, and S. R. Forrest: Appl. Phys. Lett. **88** (2006) 233502.
9) G. Li, Y. Yao, H. Yang, V. Shrotriya, G. Yang, and Y. Yang: Adv. Funct. Mater. **17** (2007) 1636.
10) F. C. Chen, C. J. Ko, J. L. Wu, and W. C. Chen: Sol. Energy Mater. Sol. Cells **94** (2010) 2426.
11) C. J. Brabec, S. E. Shaheen, C. Winder, N. S. Sariciftci, and P. Denk: Appl. Phys. Lett. **80** (2002) 1288.
12) J.-L. Wu, F.-C. Chen, M.-K. Chung, and K.-S. Tan: Energy Environ. Sci. **4** (2011) 3374.